P. Reynolds, R. J. Brown, T. Thordarson, E. W. Llewellin, K. Fielding

Rootless cone eruption processes informed by dissected tephra deposits and conduits

Bulletin of Volcanology, 2015; 77(9): 72-1-72-17

Rootless cone eruption processes informed by dissected tephra deposits and conduits

P. Reynolds[1*], R. J. Brown[1], T. Thordarson[2], E.W. Llewellin[1], K. Fielding[3]

[1]Department of Earth Sciences, Durham University, Science Labs, Durham, DH1 3LE, UK

[2]Faculty of Earth Sciences and Nordvulk, University of Iceland, Sturlugata 7, 101 Reykjavík, Iceland

[3]Formerly at: Hess Corporation, Level 9, The Adelphi Building, 1-1 John Adam Street, London, WC2N 6AG, UK

*Corresponding author: peter.reynolds@durham.ac.uk, +447887863550

Abstract

Rootless cones result from the explosive interaction between lava flows and underlying water-saturated sediment or volcaniclastic deposits. Rootless explosions can represent a significant far-field hazard during basaltic eruptions, but there are few detailed studies of their deposits. A rootless cone field in the 8.5 Ma Ice Harbor flow field of the Columbia River Basalt Province, NW USA, is revealed by sections through rootless conduit and cone structures. The Ice Harbor lava flow hosting the rootless cones was emplaced across a floodplain or lacustrine environment that had recently been mantled by a layer of silicic volcanic ash from a major explosive eruption. Our observations indicate a two-stage growth model for the rootless cones: (1) initial explosions generated sediment-rich tephra emplaced by fallout and pyroclastic density currents; and (2) later weaker explosions that generated spatter-rich fountains. Variable explosive activity resulted in a wide range of pyroclast morphologies and vesicularities. Cross-sections through funnel-shaped conduits also show how the conduits were constructed and stabilised. The growth model is consistent with decreasing water availability with time, as inferred for rootless cones described in Iceland. The Ice Harbor rootless cones provide further lithological data to help distinguish between rootless cone-derived tephra and tephra generated above an erupting dyke.

Keywords: rootless cones; basalt lava; pāhoehoe; Columbia River Basalt Province; lava-water interaction.

1. Introduction

Explosive interaction between water-logged sediments (or volcaniclastic deposits) and molten lava can result in the formation of rootless cones, also known as 'pseudocraters' (Fig. 1; Thorarinsson 1953). Rootless cones are present within flow fields where the lava advanced over lacustrine, marsh and fluvial environments (Fagents and Thordarson 2007; Hamilton et al. 2010a, 2010b). Explosions are driven by the interaction of molten lava with a water-saturated, unconsolidated substrate. Explosions initiated by interaction of molten lava with substrate pore water eject clasts composed of lava crust, disrupted liquid lava and substrate-derived sediment onto a stationary surface of an active lava flow, thereby building a cone. Similar rootless edifices, known as littoral cones, form when lava flows interact with seawater in a littoral environment (Moore and Ault 1965; Fisher 1968; Jurado-Chichay et al. 1996; Mattox and Mangan 1997; Jaeger et al. 2007). Rootless cone-like structures have also been observed on the surface of Mars near the Martian equator (Lanagan et al. 2001; Bruno et al. 2004; Fagents and Thordarson 2007; Hamilton et al. 2010a) and have been used to infer the former presence of fluids in the Martian substrate.

Two models for rootless eruptions have been proposed; one assuming static heat transfer and the other inferring dynamic heat transfer. The static heat transfer model infers rapid emplacement of lava above a water-logged substrate. Water trapped beneath the lava flow is converted to steam producing eruptions that are analogous to phreatic explosions (Thorarinsson 1951, 1953).

In contrast, the dynamic heat transfer model of Fagents and Thordarson (2007) argues that the explosive interactions are driven by physical (dynamic) mixing of the lava and the water-logged substrate. The model is based on observations that sediment from the substrate is physically mixed into the rootless cone deposits and found between the core and the rim in armoured bombs. Furthermore, the cones feature multiple layers of tephra, which increase upwards in grain size from coarse ash/fine lapilli to bomb-size clasts (Fagents and Thordarson 2007; Hamilton et al. 2010). The presence of layering implies sustained eruptions (estimated to have lasted for hours to days; Thordarson and Höskuldsson 2008), maintained by quasi-steady input of molten lava to the explosion site.

During rootless cone activity on pāhoehoe lavas, initial sedimentation occurs from explosions that produce pyroclastic density currents (PDCs) that deposit broad, sheet-like platform deposits around the vent (Hamilton et al. 2010a). Later tephra jets and lava fountains deposit lapilli- to bomb-sized scoria and spatter that build a cone (Thordarson et al. 1998; Fagents and Thordarson 2007; Hamilton et al. 2010a). The deposits of rootless activity are usually unconsolidated, except in proximal regions (Hamilton et al. 2010a). Rootless cones vary from 1−40 m in height and 2−450 m in basal diameter. The cones are crudely bedded, inversely graded, and may contain layers of rheomorphic spatter. The degree of explosivity is thought to be controlled by the explosion site geometry, the rate of lava influx, and the amount and availability of external water. Tephra deposits within rootless cone fields can cover areas of up to 150 km^2 and may exhibit complex stratigraphic relationships (Fagents and Thordarson 2007; Hamilton et al. 2010a and references therein).

Despite the abundance of rootless cones (e.g. Greeley and Fagents 2001; Lanagan et al. 2001; Fagents et al. 2002; Bruno et al. 2004; Fagents and Thordarson 2007; Hamilton et al. 2010a, 2010b, 2010c, 2011; Keszthelyi and Jaeger 2014), there is little documentation of their constituent pyroclasts and the characteristics of their host lava flows (e.g. Melchior Larsen et al. 2006; Hamilton et al. 2010a; 2010 b). Furthermore, rootless cones are superficially similar to small scoria cones and spatter cones, both in size and componentry (e.g. Fagents and Thordarson 2007). They may also have a linear spatial arrangement, similar to that of edifices along a dyke (e.g. Hamilton et al. 2010a). The limited knowledge of the internal stratigraphy of rootless cones coupled with their similarity to other volcanic edifices means that it can be difficult to distinguish rootless tephra from tephra generated during dyke-fed eruptions. This is particularly the case in flood basalt provinces, where pyroclastic successions are usually poorly preserved and poorly exposed (e.g. Swanson et al. 1975; Reidel and Tolan 1992; Brown et al. 2014).

In this paper, we document a newly discovered rootless cone field within the 8.5 Ma Ice Harbor pāhoehoe lava flow field in the Columbia River Basalt Province (CRBP), USA. Erosional dissection allows us to examine the tephra deposits and conduits of the rootless cones. We use these features to inform on the nature of the explosions that created the rootless cones and to help define criteria that distinguish the deposits of rootless cones from those of dyke-fed eruptions.

2. Geological setting of the Columbia River Basalt Province

Flood basalt volcanism in the NW USA initiated c. 17 m.y. ago in the Steens Mountain region, Oregon. Over the following ~11 m.y. the volume of erupted mafic magma exceeded >210 000 km^3 across Oregon and Washington (now considered part of the CRBP; Camp et al. 2003; Reidel et al. 2013). Eruptions were fed by ~300 km-long dyke swarms from crustal magma chambers under east-central Oregon/west-central Idaho (Wolff et al. 2008; Ramos et al. 2013). Volcaniclastic rocks in the CRBP are generally scarce, although exceptionally preserved examples of proximal tephra deposits (Swanson et al. 1975; Reidel and Tolan 1992; Brown et al. 2014), hyaloclastite deposits (Tolan et al. 2002), inferred rootless deposits (Thordarson and Self 1998) and drowned rootless cones (Keszthelyi and Jaeger 2014) are known.

The rootless cone deposits in this study occur in the 8.5 Ma Ice Harbor Member (Fig. 2), which is composed of three pāhoehoe lava flow fields that are the youngest products ascribed to the CRBP (McKee et al. 1977; Swanson et al. 1979). The lavas have been divided into three chemically distinct types that were fed from a dyke system that was up to 90 km in length and on average <15 km in width (Swanson et al. 1975). The lava flow field has a minimum volume of 1.2 km^3 (Swanson et al. 1975) and individual lava flows are typically <15 m thick. The pāhoehoe lavas are interbedded with the Ellensburg Formation sediments – diatomaceous muds, lacustrine sands and silts, volcaniclastic silt, conglomerates, and silicic volcanic ash probably sourced from eruptions of volcanoes in the NW USA. These sediments record deposition both within extensive lava-dammed lakes and by ephemeral and established rivers (Schminke 1967; Smith 1988; Tolan et al. 2002).

3. Method

Field studies involved detailed sedimentary logging of tephra successions, lithofacies analysis, geological mapping and sampling. Locations were recorded using a handheld GPS unit with an accuracy of ±5 m. Petrographic characterisation was undertaken by optical microscopy on representative thin sections. Vesicle and clast dimensions and abundances were calculated using the image analysis software ImageJ (http://imagej.nih.gov/ij/) with representative samples and outcrop photographs. The crystal content of the cone deposits was calculated by point-counting representative samples. Clast densities were calculated on clasts >16 mm across using the method of Houghton and Wilson (1989). Grain size was determined by sieving.

4. Ice Harbor rootless cone field

The Ice Harbor rootless cone field is composed of: 1) the substrate over which the lava flows were emplaced (silicic volcanic ash); 2) the host pāhoehoe lava flows; 3) rootless cone conduits within the lava flows; 4) rootless cone- and platform-forming tephra deposits. The cone field is inferred to have occupied an area of ≥1 km^2, based on the distribution of the conduits and associated tephra. The cone field is overlain by later Ice Harbor lava flows.

4.1 Volcanic ash substrate

The pre-eruption substrate beneath the Ice Harbor flow field does not crop out in the study area, and the nature of the substrate has been inferred from analysis of material incorporated into the rootless cone tephra deposits. This material is composed of white, silicic, volcanic ash and forms 10–85 vol. % of all rootless cone tephra deposits. The volcanic ash is well-sorted (1.2 $\sigma\Phi$) and individual particles are platy, angular or cuspate in shape and occasionally preserve vesicles. The volcanic ash has a median diameter of <0.25 mm. Smaller particles are blade shaped, whilst coarser particles have complex morphologies and exhibit bubble junctures.

Interpretation

The silicic volcanic ash is interpreted as a pyroclastic fall deposit within the Ellensburg Formation (e.g. Schminke 1967). The monolithologic character of the volcanic ash and the absence of organic matter or detrital sediment indicate that the volcanic ash had not been substantially reworked and that burial by the Ice Harbor lava may have occurred shortly after fallout. We infer that the volcanic ash fell out onto a flood plain or shallow lake; common features across the plateau-like CRBP during the Miocene (e.g. Schminke 1967; Smith 1988; Tolan et al. 2002). These environments are conducive to the formation of rootless cones (e.g. Thorarinsson 1951, 1953; Fagents and Thordarson 2007; Hamilton et al. 2010a, 2010b).

4.2 Ice Harbor lava flows

The rootless cone field crops out along the banks of the Snake River (Fig. 2). The flow field is composed of pāhoehoe sheet lobes that reach 8 m thick and exhibit the tripartite structure typical of pāhoehoe sheet lobes in the CRBP (e.g. Self et al. 1998; Thordarson and Self 1998). They have lower crusts that contain distorted pipe vesicles, massive, dense cores with columnar joints and vesicular upper crusts. The groundmass of the flows is composed of interstitial glass, and plagioclase and pyroxene microlites. Pyroxene and rare swallow-tail plagioclase phenocrysts and glomerocrysts 0.1−3 mm in diameter constitute 1−4 vol. % of the rock. Vesicles are partially filled with zeolite minerals. The Ice Harbor sheet lobes that contain the rootless cones have poorly vesicular cores and incipiently vesicular crusts (as defined by Houghton and Wilson 1989) that exhibit hackly, entablature-style joints spaced 11–21 cm apart.

Interpretation

We infer that inflation of the flows took several weeks, based on a lava upper crust thickness of ≥2 m and the relationship: $t = 164.8C^2$; where t= time in hours and C=crustal thickness in metres (see Hon et al. 1994). The presence of entablature-style jointing in the lava indicates that the flows were subjected to water enhanced cooling, implying emplacement in an environment where surface water was abundant (e.g. Long and Wood 1986). The swallow tail plagioclase microlites indicate that the lava cooled rapidly; this texture is also found in pillow lavas (e.g. Bryan 1972; Jafri and Charan 1992).

4.3 Rootless cone conduits

Cliffs along the Snake River reveal funnel-shaped, upward-flaring features in the Ice Harbor sheet lobes (Fig. 3). These features range from 1–4 m in diameter, are up to 4 m deep and have cross-sectional areas of 8–12 m². Their walls dip inwards ~60˚. All the funnels appear to terminate ≥0.5 m above the bases of the sheet lobes and sometimes form irregular, isolated cavities; these are likely 2D section effects (Fig. 3). Hackly cooling joints spaced ~16 cm apart radiate away from the funnel walls and extend up to ~4 m into the surrounding lava core (Fig. 3).

The inner surfaces of the funnels are coated with ropey-textured and bread-crusted spatter that is ≤6 cm thick. The spatter has a hypohyaline groundmass texture, contains sheared vesicles and has multiple chilled rinds. The surface of the spatter has angular, hypocrystalline and hypohyaline clasts of upper lava crust embedded in it. These clasts cover 10–30% of each funnel wall. There is a patchy, heterogeneous distribution of silicic volcanic ash across the surfaces; typically <5%. These funnels are often partially filled with tephra with a similar composition to the overlying cone deposits (massive spatter bombs, mSp; see below).

Twelve of these features have been recognised along a 450 m transect (Fig. 2); five on the north bank of the river and seven on the south. The features are spaced 3–206 m apart with tephra deposits exposed above them. Exposures spaced less than 5 m apart may represent irregular sections through the same feature.

Interpretation

We interpret these funnel-shaped features as remnants of rootless conduits because they have spatter, angular lapilli and patches of silicic ash plastered onto their inner wall which can only have occurred via explosive interactions. They are also filled with lapilli- to bomb-sized tephra. These features distinguish them from features described within rubbly pāhoehoe flows (e.g. Duraiswami et al. 2008; Keszthelyi et al. 2009). Sheared vesicles and rope-like textures on the conduit wall result from rheomorphic flow of spatter. The funnel shape of the conduits and their radiating cooling joints are similar to features seen in rootless cones in Iceland (e.g. Hamilton et al. 2010a).

Based on the abundance of conduits and the possibility that some locations represent irregular cross sections through the same conduit (e.g. L16/17; L1/2/6; L12/13) we suggest that the flow field hosted at least eight rootless cones. Since the size of the conduits is proportional to the size of the overlying cone (e.g. Hamilton et al. 2010a), the cones were likely to have been ≥5 m in basal diameter.

4.4 Rootless cone tephra deposits

Proximal rootless platform and cone-forming deposits are widely exposed over a 450 m-long transect along the south bank of the Snake River, and are intermittently exposed along the north bank of the river (Fig. 2). The tephra deposits are composed of juvenile pyroclasts (described below), silicic volcanic ash and fragmented lava crust.

4.4.1 Juvenile pyroclast types

The tephra deposits contain four different pyroclast types derived from the fragmentation and modification of the host lava flow (Fig. 4; Table 1). These juvenile clasts are (1) sideromelane ash and lapilli of both blocky and fluidal morphologies; (2) hypocrystalline bombs (with both ventricular and globular morphologies) and angular lapilli; (3) armoured scoria bombs and lapilli; and (4) spatter bombs. All clasts have hypohyaline to hypocrystalline groundmasses and are mineralogically similar to the host lava. The pyroclasts are incipiently to poorly vesicular, ranging between 15–36% vesicles, and are non to incipiently welded. The density of pyroclasts ranges from 1700–2300 kg m^{-3}. The pyroclast types and their occurrence is summarised in Table 1.

Interpretation

The density of the Ice Harbor rootless tephra is significantly higher than that of non-welded basaltic pyroclasts produced during dyke-fed eruptions (typically 240–1440 kg m^{-3}; Houghton and Wilson 1989; Parcheta et al. 2013). This suggests that the pyroclasts were sourced from lava that had already degassed at the source fissure and during transport to the rootless cone site. The ventricular and globular bombs are atypical of the deposits of fissure eruptions (e.g. Valentine and Gregg 2008); they are interpreted as water-quenched globules of lava ejected from beneath the lava flow during explosive activity. These bombs were subsequently mechanically fragmented into angular lapilli upon eruption and deposition, enhanced by cooling contraction fractures. The spatter bombs are interpreted as proximal deposits from rootless lava fountains (e.g. as observed during the 1783−1785 Laki eruptions, see Thordarson et al. 1998). Recycling by intermittent fountains appears necessary to form the armoured bombs. The blocky sideromelane clasts indicate cooling-contraction granulation and/or mechanical fragmentation. The fluidal, elongate sideromelane clasts indicate ductile disruption of molten lava and are common components of deposits from magmatic volatile driven eruptions (e.g. Walker and Croasdale 1971), phreatomagmatism (e.g. Zimanowski et al. 1997; Morrissey et al. 2000; Büttner et al. 2002) and peperite (see section 4.4.3; Skilling et al. 2002).

4.4.2 Pyroclastic lithofacies

The tephra deposits can be sub-divided into four lithofacies according to their componentry, grain size and depositional structures (Fig. 5; Table 2). In general the pyroclastic lithofacies appear moderately to very poorly sorted and are composed of juvenile clasts with <10–85 vol. % silicic volcanic ash. Lithofacies with the largest juvenile clasts tend to have the least silicic volcanic ash (Fig. 6). The lithofacies form proximal platform, cone or conduit-filling deposits.

Sheet deposits are not found; these are commonly unconsolidated (Hamilton et al. 2010a). Contacts between the tephra deposits and underlying lavas are not exposed (Fig. 6).

Platform deposits include massive or normally graded lapilli-ash (m/nLAf), lenses of lapilli-ash (lensLA) and cross-stratified lapilli-ash (xsLA; Table 2; Fig. 5). These deposits are 1–5.5 m in thickness (Fig. 7) and are present beneath the parallel-bedded spatter (//bSp; Figs. 6 and 7). Pyroclasts within the deposits are dominantly of lapilli size. They are exposed over a ~600 m long transect. Bedding dips vary from 10–20˚.

Cone deposits are composed of parallel-bedded spatter (//bSp; Table 2) that is 1–3 m thick (Fig. 6) and contains predominantly bomb-sized clasts. Deposits are exposed over a ~200 m long transect. The spatter varies from horizontally bedded to dipping up to 20˚; whether this is towards or away from a conduit is unclear (Figs. 6 and 7).

The conduits are partially filled with massive spatter (mSp; Table 2) and are not observed in contact with overlying cone and/or platform deposits.

Interpretation

The Ice Harbor platform deposits are inferred to have been deposited from both PDCs and by fallout (e.g. Hamilton et al. 2010a). The occurrence of massive/normally graded lapilli-ash (m/nLAf), lenses of lapilli-ash (lensLA) and cross-stratified lapilli-ash (xsLA) beneath the spatter-rich deposits (e.g. //bSp) suggests that the platform was constructed prior to cone formation. Intermittent deposits of normally-graded lapilli ash (nLA) and cross-stratified lapilli-ash (xsLA; Fig. 6) overlying the spatter layers suggests that the cone field is composed of numerous overlapping cones formed in a sequence of rootless eruptions (e.g. Fagents and Thordarson 2007). The thickness and spatial distribution of the exposures suggest that the tephra platforms were ~5 m thick and were likely to be laterally extensive over 100's of metres. Cone-forming and conduit-filling deposits of rootless cones commonly contain spatter-rich lithofacies (Hamilton et al. 2010a), as observed in this study. These coarse-grained deposits are produced as the explosivity of the eruptions decreases (Fagents and Thordarson 2007).

4.4.3 Lava-silicic volcanic ash interaction textures in tephra deposits

A variety of peperite-like textures are observed in the tephra deposits (Fig. 8). Fluidal textures include spatter bombs that inter-finger with the silicic volcanic ash and associated globular and elongate spatter lapilli and ash found intimately mixed with the silicic volcanic ash. Within 2 cm of the spatter, the silicic volcanic ash is often thermally altered, becoming dark in colour and fused (e.g. Schminke 1967). Where fused, the silicic volcanic ash contains vesicles ≤2 mm in diameter. Vesicles in the spatter also contain silicic ash. Blocky textures include jigsaw-fit bombs; these clasts have hairline fractures filled with silicic volcanic ash. Other bombs have rinds that are partially separated from their core, encapsulating a 2 mm-thick domain of silicic volcanic ash between rind and core. These domains contain mm-scale globules of lava.

Interpretation

Peperite-like textures indicate interaction between hot juvenile clasts and unconsolidated sediment (e.g. Skilling et al. 2002). Vesicles in the fused silicic volcanic ash indicate that gas was generated during interaction (e.g. Kokelaar 1982; Skilling 2002; Squire and McPhie 2002). Silicic ash-filled vesicles in the spatter indicate that the sediment was mobilised during interaction (e.g. Goto and McPhie 1996: Skilling 2002 and references there-in). The fluidal and blocky textures indicate variations in mechanical stress, movement of lava, lava-silicic ash density contrasts and variations in lava viscosity and clast size (e.g. Skilling et al. 2002; Squire and McPhie 2002). These textures may represent a failed phreatomagmatic fragmentation process formed beneath the lava flow (e.g. Busby-Spera and White 1987; Hooten and Ort 2002). The bombs with encapsulated silicic volcanic ash are interpreted as intrusions of lava into the underlying substrate. Lava globules in the silicic volcanic ash domain indicate that the cores of these bombs were molten during intrusion.

5. Emplacement of the Ice Harbor rootless cones

We infer that the Ice Harbor lava flows traversed a lacustrine or floodplain environment (Fig. 9). The ground was mantled by a layer of silicic volcanic ash fall derived from a major explosive eruption. As the lava flows inflated they developed brittle basal crusts (Hon et al. 1994). These crusts were weakened by the development of cooling fractures (Thordarson and Self 1998) which created a zone of weakness along the base of the flows. Cracking and subsequent failure of the crust would have been facilitated by heterogeneous subsidence of the flows during inflation (e.g. Fagents and Thordarson 2007; Hamilton et al. 2010a). Failure of the basal crust allowed extrusion of lava, analogous to the axial cleft of a tumulus (e.g. Walker 1991; Rossi and Gudmundsson 1996; Hamilton et al. 2010a).

Extrusion of lava through the basal crust resulted in the intimate mixing of molten lava with the water-saturated silicic volcanic ash. This mixing of the lava and sediment is evidenced by the peperite-like textures and abundance of silicic volcanic ash (i.e. substrate) in the tephra deposits. Lava-substrate mixing was followed by explosions. These fragmented the lower lava crust and burst through the molten lava core creating transient conduits. The preservation of conduits requires the cooling and solidification of the conduit walls over time to prevent pressure-driven collapse of the walls between explosions. The presence of spatter lining the walls of the conduits indicates that they were stabilised from both material ejected during the explosions, as well as from the chilling of the molten lava core. Explosive activity deposited the massive/normally graded lapilli-ash (lithofacies m/nLA (f)) on top of the lava flow. Some of the pyroclastic material formed PDCs (depositing lithofacies lensLA and xsLA; Table 2). These processes constructed the tephra platforms.

Spatter-rich lithofacies (e.g. //bSp and mSp; Table 2) were produced during rootless lava fountaining and cap the rootless cone successions and fill some conduits. The coarse clast size of these lithofacies indicates decreasing explosivity as water availability declined. Explosions also embedded juvenile clasts and lava crust lithics into the hot and ductile conduit walls.

The presence of the cones on top of sheet lobes suggests that the cones developed repelled, non-aligned spatial distributions (e.g. Hamilton et al. 2010a, 2010b). The cones were likely to have formed in topographic lows where lava and water were most abundant, and in regions of enhanced substrate compressibility (Hamilton et al. 2010a, 2010b). Exposures do not allow determination of the symmetry of the cones (e.g. radial or elongate). Growth of the cones was terminated by the decreasing availability of ground water, or by water being prevented from gaining access to the explosion site. Continued cooling stabilised the conduit walls and over time cooling joints radiated out into the core (e.g. Fig. 9).

6. Comparison with other rootless cones

The deposits in this study are comparable with the platform and cone-building deposits of rootless cones in Iceland (e.g. Table 3; Fig. 10), which show a similar pattern of sediment-rich PDC deposits overlain by coarse-grained fall deposits. These PDC and fall deposits are composed of scoria lapilli and bombs, spatter bombs and clastogenic lava, all intimately mixed with silt- to cobble-sized sediment. The coarse grainsize of the platform deposits in this study relative to others described in Iceland (Hamilton et al. 2010a) may result from the proximity of the Ice

Harbor tephra platforms to the explosion source, or from less efficient magma-water interaction. The substrate properties (e.g. grainsize distribution and thermal conductivity) may also have affected explosivity (e.g. Sohn 1996; White 1996). Furthermore, the properties of the substrate would have evolved during the eruptions, due to mixing of pyroclasts and silicic volcanic ash beneath the lava flow. However, the role of sediment properties in governing the explosivity of rootless eruptions is as-yet unknown.

7. Conclusions

The Ice Harbor tephra deposits provide insights into the construction and componentry of a rootless cone field. Cross sections of conduits suggest that ≥8 cones were present in a cone field ≥1 km^2 in area. Cone- and platform-forming deposits are composed of admixed juvenile clasts, clasts from the host lava flow and silicic volcanic ash from an earlier, major explosive eruption in NW USA. Construction of the cone field occurred through a combination of deposition from PDCs and lava fountaining. Explosivity decreased with time as a result of decreasing water availability in the underlying silicic volcanic ash. This study demonstrates that the abundance of sediment (in this case, silicic volcanic ash) in the tephra, juvenile clast morphology and clast density are useful criteria for distinguishing between rootless tephra and tephra produced above an erupting dyke.

Acknowledgements

PR acknowledges a studentship funded by Hess Corporation as part of the Volcanic Margins Research Consortium. Reviewers Bernd Zimanowski and Laszlo Keszthelyi are thanked for their thoughtful input, as is associate editor Pierre-Simon Ross.

References

Brown RJ, Blake S, Thordarson T, Self S (2014) Pyroclastic edifices record vigorous lava fountains during the emplacement of a flood basalt flow field, Roza Member, Columbia River Basalt Province, USA. Geol Soc Am Bull 126:875-891

Bruno BC, Fagents S, Thordarson T, Baloga SM, Pilger E (2004) Clustering within rootless cone groups on Iceland and Mars: Effect of nonrandom processes. J Geophys Res 109:1991-2012

Bryan WB (1972) Morphology of quench crystals in submarine basalts. J Geophys. Res. 77:5812-5819

Busby-Spera CJ, White, JD (1987) Variation in peperite textures associated with differing host-sediment properties. B Volcanol 49:765-776

Büttner R, Dellino P, La Volpe L, Lorenz V, Zimanowski B (2002) Thermohydraulic explosions in phreatomagmatic eruptions as evidenced by the comparison between pyroclasts and products from Molten Fuel Coolant Interaction experiments. J. Geophys. Res. 107:2277

Camp VE, Ross ME, Hanson WE (2003) Genesis of flood basalts and Basin and Range volcanic rocks from Steens Mountain to the Malheur River Gorge, Oregon. Geol Soc Am Bull 115:105-128

Duraiswami RA, Bondre NR, Managave S (2008) Morphology of rubbly pahoehoe (simple) flows from the Deccan Volcanic Province: Implications for style of emplacement. J Volcanol Geotherm Res 177:822-836

Fagents SA, Thordarson T (2007) Rootless cones in Iceland and on Mars. In: Chapman M, Skilling IP (eds) The Geology of Mars: Evidence from Earth-Based Analogues. Cambridge University Press, pp 151–177

Fagents SA, Lanagan P, Greeley R (2002) Rootless cones on Mars: a consequence of lava-ground ice interaction. Geological Society, London, Special Publications 202:295-317

Fisher RV (1968) Puu Hou littoral cones, Hawaii. Geologische Rundschau 57:837-864

Goto Y, McPhie J (1996) A Miocene basanite peperitic dyke at Stanley, northwestern Tasmania, Australia. J Volcanol Geoth Res 74:111-120

Greeley R, Fagents SA (2001) Icelandic pseudocraters as analogs to some volcanic cones on Mars. J. Geophys. Res. 106:20527-20546

Hamilton CW, Thordarson T, Fagents SA (2010a) Explosive lava–water interactions I: architecture and emplacement chronology of volcanic rootless cone groups in the 1783–1784 Laki lava flow, Iceland. B Volcanol 72:449-467

Hamilton CW, Fagents SA, Thordarson T (2010b) Explosive lava–water interactions II: self-organization processes among volcanic rootless eruption sites in the 1783–1784 Laki lava flow, Iceland. B Volcanol 72:469-485

Hamilton CW, Fagents SA, Wilson L (2010c), Explosive lava-water interactions in Elysium Planitia, Mars: Geologic and thermodynamic constraints on the formation of the Tartarus Colles cone groups, J. Geophys. Res. 115:1991-2012

Hamilton CW, Fagents SA, Thordarson T (2011) Lava–ground ice interactions in Elysium Planitia, Mars: Geomorphological and geospatial analysis of the Tartarus Colles cone groups, J. Geophys .Res. 116:1991-2012

Hon K, Kauahikaua J, Delinger R, Mackay K (1994) Emplacement and inflation of pahoehoe sheet flows: Observations and measurements of active lava flows on Kilauea Volcano, Hawaii. Geol Soc Am Bull 106:351-370

Hooten JA, Ort MH (2002) Peperite as a record of early-stage phreatomagmatic fragmentation processes: an example from the Hopi Buttes volcanic field, Navajo Nation, Arizona, USA. J Volcanol Geoth Res 114:95-106

Houghton BF, Wilson CJN (1989) A vesicularity index for pyroclastic deposits. B Volcanol 51:451-462

Jaeger WL, Keszthelyi LP, McEwen AS, Dundas CM, Russell PS (2007) Athabasca Valles, Mars: A Lava-Draped Channel System. Science 317:1709-1711

Jafri SH, Charan SN (1992) Quench textures in pillow basalt from the Andaman-Nicobar Islands, Bay of Bengal, India. Proc. Indian Acad. Sci. (Earth Planet Sci) 101:99-107

Jurado-Chichay Z, Rowland S, Walker GL (1996) The formation of circular littoral cones from tube-fed pāhoehoe: Mauna Loa, Hawai'i. B Volcanol 57:471-482

Keszthelyi LP, Jaeger WL (2014) A field investigation of the basaltic ring structures of the Channeled Scabland and the relevance to Mars. Geomorph, doi:10.1016/j.geomorph.2014.06.027

Keszthelyi LP, Baker VR, Jaeger WL, Gaylord DR, Bjornstad BN, Greenbaum N, Self S, Thordarson T, Porat N, Zreda MG (2009) Floods of water and lava in the Columbia River Basin: Analogs for Mars. Geol Soc Am Field Guides 15:845-874.

Kokelaar BP (1982) Fluidization of wet sediments during the emplacement and cooling of various igneous bodies. J Geol Soc 139:21-33

Lanagan PD, McEwen AS, Keszthelyi LP, Thordarson T (2001) Rootless cones on Mars indicating the presence of shallow equatorial ground ice in recent times. Geophys Res Lett 28:2365-2367

Long PE, Wood BJ (1986) Structures, textures, and cooling histories of Columbia River basalt flows. Geol Soc Am Bull, 9:1144-1155.

Mattox TN, Mangan MT (1997) Littoral hydrovolcanic explosions: a case study of lava–seawater interaction at Kilauea Volcano. J Volcanol Geoth Res 75:1-17

McKee E, Swanson D, Wright T (1977) Duration and volume of Columbia River basalt volcanism, Washington, Oregon and Idaho. In: Geol. Soc. Am. Abstr. Programs. pp 463-464

Melchior Larsen L, Ken Pedersen A, Krarup Pedersen G (2006) A subaqueous rootless cone field at Niuluut, Disko, Paleocene of West Greenland. Lithos 92:20-32

Moore JG, Ault WU (1965) Historic littoral cones in Hawaii. Pacific science XIX(3-11)

Morrissey M, Zimanowski B, Wohletz KH, Buettner R (2000) Phreatomagmatic fragmentation. In: Sigurdsson H (ed) Encyclopedia of volcanoes, pp 431-445.

Parcheta CE, Houghton BF, Swanson DA (2013) Contrasting patterns of vesiculation in low, intermediate, and high Hawaiian fountains: A case study of the 1969 Mauna Ulu eruption. J Volcanol Geoth Res 255:79-89

Ramos FC, Wolff JA, Starkel W, Eckberg A, Tollstrup DL, Scott S (2013) The changing nature of sources associated with Columbia River flood basalts: Evidence from strontium isotope ratio variations in plagioclase phenocrysts. Geol Soc Am Spec Pap 497:231-257

Reidel SP, Tolan TL (1992) Eruption and emplacement of flood basalt: An example from the large-volume Teepee Butte Member, Columbia River Basalt Group. Geol Soc Am Bull 104:1650-1671

Reidel SP, Camp VE, Tolan TL, Martin BS (2013) The Columbia River flood basalt province: stratigraphy, areal extent, volume, and physical volcanology. Geol Soc Am Spec Pap 497:1-43

Rossi MJ, Gudmundsson A (1996) The morphology and formation of flow-lobe tumuli on Icelandic shield volcanoes. J Volcanol Geotherm Res 72:291–308

Schminke H-U (1967) Fused Tuff and Pépérites in South-Central Washington. Geol Soc Am Bull 78:319-330

Self S, Keszthelyi L, Thordarson T (1998) The importance of pahoehoe. Annu. Rev. Earth Planet. Sci. 26:81-110

Simpson K, McPhie J (2001) Fluidal-clast breccia generated by submarine fire fountaining, Trooper Creek Formation, Queensland, Australia. J Volcanol Geoth Res 109:339-355

Skilling IP, White JDL, McPhie J (2002) Peperite: a review of magma–sediment mingling. J Volcanol Geoth Res 114:1-17

Smith GA (1988) Neogene synvolcanic and syntectonic sedimentation in central Washington. Geol Soc Am Bull 100:1479-1492

Sohn YK (1996) Hydrovolcanic processes forming basaltic tuff rings and cones on Cheju Island, Korea. Geol Soc Am Bull 108:1199-1211

Sumner JM, Blake S, Matela RJ, Wolff JA (2005) Spatter. J Volcanol Geoth Res 142(1-2):49-65

Swanson DA, Wright TL, Helz RT (1975) Linear vent systems and estimated rates of magma production and eruption for the Yakima Basalt on the Columbia Plateau. Am J Sci 275:877-905

Swanson D, Wright TL, Hooper PR, Bentley RD (1979) Revisions in stratigraphic nomenclature of the Columbia River Basalt Group. U.S Geol Surv Bull 1457 G1-G59

Thorarinsson S (1951) Laxargljufur and Laxarhraun: a tephrochronological study. Geograf Annal 2:1−89

Thorarinsson S (1953) The crater groups in Iceland. B Volcanol 14:3-44

Thordarson T, Self S (1998) The Roza Member, Columbia River Basalt Group: A gigantic pahoehoe lava flow field formed by endogenous processes? J. Geophys. Res. 103:27411-27445

Thordarson T, Höskuldsson Á (2008) Postglacial volcanism in Iceland. Jökull 58:197-228.

Thordarson T, Miller D, Larsen G (1998) New data on the Leidolfsfell cone group in South Iceland. Jökull 46: 3-15

Tolan TL, Beeson MH, Lindsey KA (2002) The effects of volcanism and tectonism on the evolution of the Columbia River system. In: A Field Guide to Selected Localities in the South-western Columbia River Plateau and Columbia River Gorge of Washington and Oregon State. Northwest Geological Society

Valentine GA, Gregg TKP (2008) Continental basaltic volcanoes – Processes and problems. J Volcanol Geoth Res 177:857-873

Walker GPL (1991) Structure, and origin by injection of lava under surface crust, of tumuli, `lava rises´, `lava-rise pits´, and `lava inflation clefts´ in Hawaii. B Volcanol 53:546–558

Walker GPL, Croasdale R (1971) Characteristics of some basaltic pyroclastics. Bulletin Volcanologique, 35:303-317

White JDL (1996) Impure coolants and interaction dynamics of phreatomagmatic eruptions. J Volcanol Geoth Res 74:155-170

Wolff J, Ramos F, Hart G, Patterson J, Brandon A (2008) Columbia River flood basalts from a centralized crustal magmatic system. Nat Geo 1:177-180

Zimanowski B, Büttner R, Lorenz V, Häfele HG (1997) Fragmentation of basaltic melt in the course of explosive volcanism. J Geophys Res 102:803-814

Figure Captions

Fig. 1 Generalised structure of a rootless cone. The cones form on active lava flows. The conduits in the host lava flow are irregular funnels that widen upwards. The upper parts of the conduits are filled with tephra. Cooling joints in the host lava flow radiate from the conduit. Cone forming deposits are composed of lapilli- to bomb-sized material that is often reversely graded and formed by fallout. Platform and sheet deposits are formed by fallout and deposition from pyroclastic density currents. Adapted from Hamilton et al. (2010a)

Fig. 2 Location of the study area. **a** The CRBP in the NW USA, adapted from Brown et al. (2014). **b** Map of the area showing the Ice Harbor fissure as described by Swanson et al. (1975) and our field area on the banks of the Snake River. **c** Sites of the tephra and conduit deposits described in this study

Fig. 3 Field photographs and schematic diagrams showing the varying geometries of rootless conduits. **a** Field sketch showing the upper part of a funnel-shaped conduit at location 6 (UTM Nad83 zone 11T, 359 987 E/5 126 647 N). View to the southwest. **b** Field photograph of massive spatter (mSp) within the conduit in **a**, composed of spatter bombs, silicic volcanic ash and hypocrystalline lapilli. **c** Irregular lower part of a conduit in the lava flow at location 22 (UTM Nad83 zone 11T, 359 724 E/5 128 162 N) with cooling joints (white) radiating from the conduit/lava core contact (outlined). The ruler is 1 m. Inset **d** shows a close up of the conduit inner wall with embedded juvenile and lava crust lithic clasts. The ruler is 25 cm. Image **e** shows a cross section through the conduit wall, with hypohyaline lapilli embedded into the surface. **f** Interpretive sketch of e. **g** Plan view of a section of conduit wall, approximately 100 mm across, showing clasts that are inferred to have become embedded in the conduit wall during explosions (dashed outlines)

Fig. 4 Clast types recognised in this study. **a** Folded spatter bomb with embedded lapilli (dashed outline). Graticules on the scale card are 1 cm (UTM Nad83 zone 11T, 359 942 E/5 126 519 N). **b** Ventricular clast (outlined). The clast has an amoeboid shape with a hypohyaline rind approx. 10 mm thick that grades inwards into the core. Vesicles up to 8 cm in diameter (dashed outline) have angular shapes and give clasts their characteristic ventricular morphology (UTM Nad83 zone 11T, 359 942 E/5 126 519 N). **c** Globular bomb (outlined). The bombs have a sub-spherical shape and a black hypohyaline rind ~1 cm thick that becomes more orange in colour toward the core. Sub angular, dull black coloured basaltic lapilli (arrowed) are contained within the cores of the bombs. Cooling joints (dashed lines) penetrate from the clast margin up to 10 mm towards the core (UTM Nad83 zone 11T, 359 942 E/5 126 519 N). **d** Armoured bomb (solid outline) with 1 cm thick dense rind and vesicular core (dashed outline) (UTM Nad83 zone 11T, 360 015 E/5 126 664 N). **e** Sideromelane clast (arrowed) formed by fragmentation in a brittle state (arrowed). **f** Sideromelane clast (arrowed) formed by ductile disruption of molten lava

Fig. 5 Lithofacies found in the study area. **a** mLA with ventricular bomb (outlined) enclosing laminated silicic volcanic ash. Graticules on the scale card are 1 cm (UTM Nad83 zone 11T, 359 881 E/5 126 506 N) **b** lensLA with hypocrystalline lapilli-rich lenses. Dashed white outlines indicate lenses (UTM Nad83 zone 11T, 359 868 E/5 126 485 N) **c** lensLA with silicic ash-rich lenses. White outlines indicate lenses (UTM Nad83 zone 11T, 359 868 E/5 126 485 N) **d** xsLA, white outlines indicate beds. The ruler is 25 cm long (UTM Nad83 zone 11T, 359 868 E/5 126

485 N) **e** //bSp, showing bedded spatter bombs. The ruler is 50 cm (UTM Nad 83 zone 11T, 359 942 E/5 126 519 N)

Fig. 6 Lithofacies logs of tephra deposits south of the river. Clast size is shown on the top axis with divisions at 32, 64, 128 and 256 mm (Location 9 uses 32, 64, 128, 256 and >1000 mm divisions). Silicic volcanic ash abundance (black squares; %) is shown across the bottom axis in 25% graticules. Logs are shown at relative altitudes. For locations of the sections see Fig. 2

Fig. 7 Photographs and interpretive pictures of Location 9 (UTM Nad 83 zone 11T, 359 942 E/5 126 519 N). **a, b** Outcrop of platform-forming admixed tephra and silicic volcanic ash. **c,d** Outcrop of cone-forming tephra composed of lithofacies //bSp

Fig. 8 Peperite-like textures produced by the interaction of juvenile clasts and silicic volcanic ash. **a** Fluidal peperite with elongate and globular clasts in lithofacies //bSp (UTM Nad 83 zone 11T, 359 942 E/5 126 519 N). **b** Blocky peperite with jigsaw-fit fractures (circled). Graticules are 1 cm (UTM Nad 83 zone 11T, 360 014 E/5 126 649 N). Thin section **c** and interpretive sketch **d** shows section of mingled spatter and silicic volcanic ash. The spatter clasts exhibit elongate and globular morphologies. The silicic ash is thermally altered and contains vesicles. Vesicles within the spatter clasts enclose silicic volcanic ash. Section of a ventricular bomb **e** and interpretive sketch **f** are also shown. The hypohyaline rind is spalling from the core and has encapsulated a domain of silicic volcanic ash. Fluidal basalt clasts are found within the silicic ash domain (arrowed) indicating that the core of the bomb was molten when the sediment was encapsulated

Fig. 9 Inferred eruption chronology for the cones. **a** Lava flow traverses wet ground and subsides heterogeneously into the underlying silicic volcanic ash. **b** Initial mingling of lava with the silicic ash results in the formation of globular and ventricular juveniles and peperite-like textures. **c** Interaction between molten lava and water saturated silicic volcanic ash results in explosive brecciation of the host lava flow and fragmentation of the globular and ventricular juveniles into lapilli and ash sized clasts. Episodic eruptions and dilute PDC's deposit poorly sorted juveniles and clasts sourced from the host lava flow, forming sheet and platform deposits (lithofacies m/nLA(f), lensLA, xsLA). Minor clast recycling may occur, producing armoured bombs. Substrate pore water is gradually depleted beneath the lava flow. **d** Decreasing water availability results in less efficient fragmentation and lava fountains are generated. These fountains produce lithofacies //bSp that builds a cone. Lapilli are also impacted into the cooling conduit walls. **e** With time water availability decreases and eruptions cease. The lava flow may continue to inflate and deform the conduit. Post-eruption cooling of the lava promotes the formation of cooling joints that radiate from the conduit

Fig. 10 Photographs of Leitin and Búrfell rootless cones in southern Iceland (UTM Nad 83, zone 27, 500 000 E/7 097 014 N; 402 187 E/7 098 548 N respectively). **a** Overlapping cone stratigraphies composed of crudely bedded spatter and scoria bombs and lapilli and clastogenic lava. The sequence is ~6 m thick. **b** Bomb-sized clast of sediment (outlined) within a sequence of scoria and spatter. The ruler is 40 cm long. **c** Sediment-rich pyroclastic density current deposit at the base of the cone forming stratigraphy. The reddish colour is given by the agglutinated sediment (inferred to be a lacustrine siltstone), not oxidation of the pyroclasts. The scale card is 120 mm long. **d** Bomb-sized, ventricular-type pyroclast (outlined) within the bedded spatter and scoria. The ruler is ~25 cm long. **e** Initial cone-forming fall deposit, composed of scoria lapilli.

Beds often form inversely-graded couplets. The bed indicated is ~6 cm thick. Beds thickness and clast size increases up-section. **f** Cross section of the conduit wall, with lapilli sized pyroclasts agglutinated to the outer wall. Cooling joints (dashed lines) radiate from the contact and are perpendicular to the conduit contact. The arrow points towards the core of the lava flow. The ruler is 30 cm long. **g** A lava flow affected by rootless cone formation. The lava flow can be divided into a colonnade (CN) and an entablature (EN), and has an irregular upper contact that forms the rootless conduit. The lava is ~10 m thick

Table 1 Summary descriptions of pyroclast types

Table 2 Summary descriptions of cone-forming and conduit deposits

Table 3 Comparison of rootless and littoral cone structures using data from Simpson and McPhie (2001); Mattox and Mangan (1997); Moore and Ault (1965); Fisher (1968); Hamilton et al. (2010a); Melchior Larsen et al. (2006); Jurado-Chichay et al. (1996); and this study

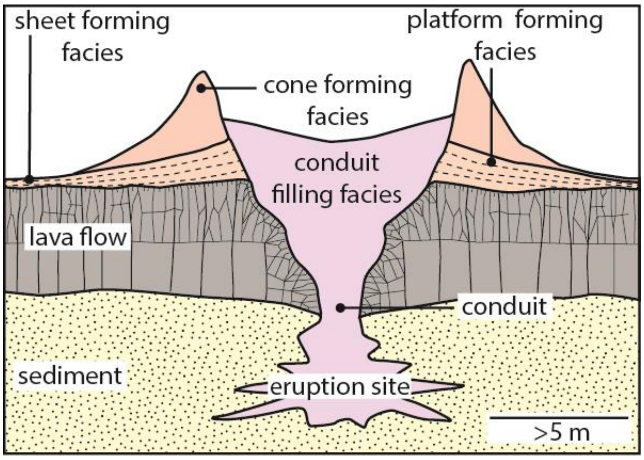
sheet forming
facies
platform forming
facies
cone forming
facies
conduit
filling facies
lava flow
conduit
sediment
eruption site
>5 m
Fig. 1

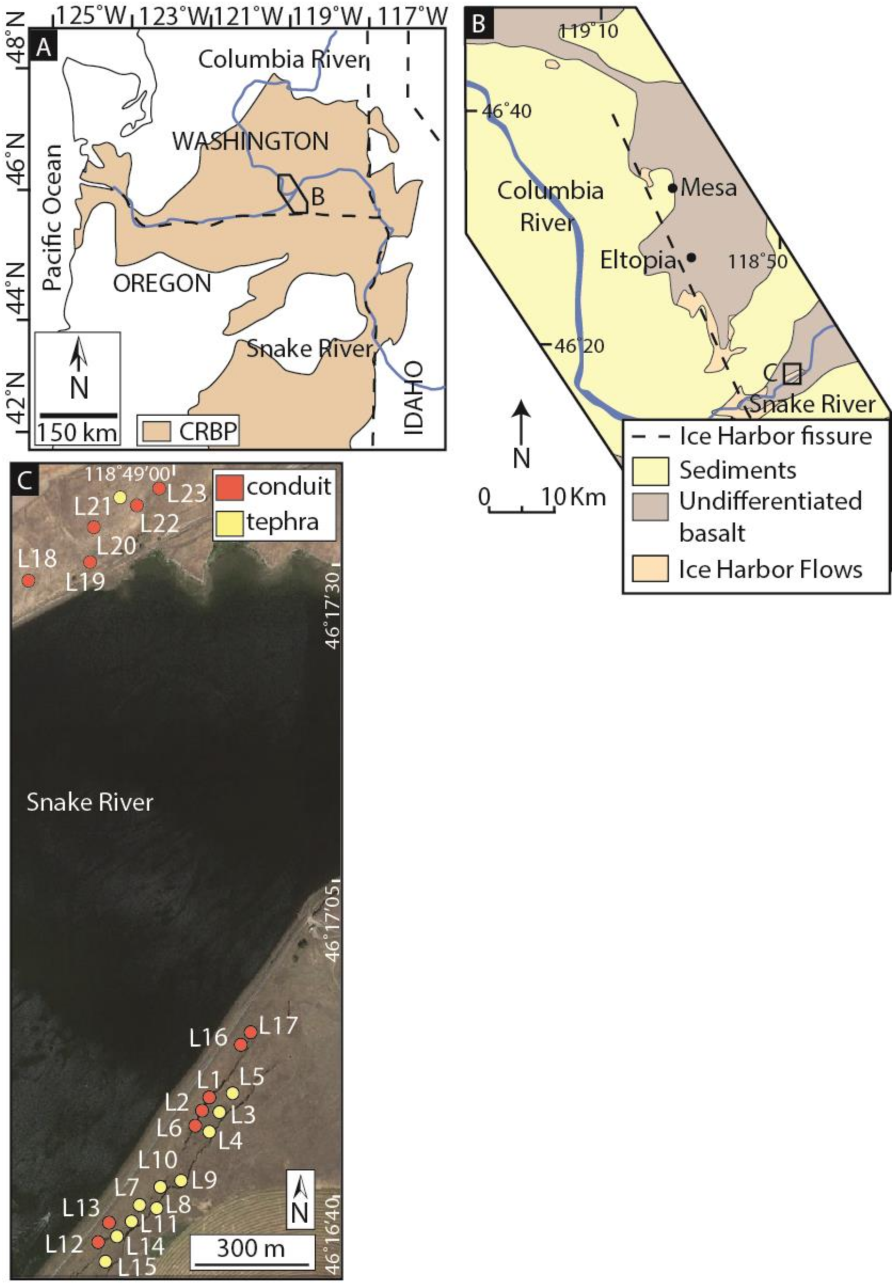
A
125°W 123°W 121°W 119°W 117°W
48°N
46°N
44°N
42°N
Columbia River
WASHINGTON
B
Pacific Ocean
OREGON
Snake River
IDAHO
N
150 km
CRBP
B
119°10
46°40
Columbia
River
Mesa
Eltopia
118°50
46°20
C
Snake River
N
0 10 Km
Ice Harbor fissure
Sediments
Undifferentiated
basalt
Ice Harbor Flows
C
118°49'00
L23
L21
L22
L20
L18
L19
conduit
tephra
46°17'30
Snake River
46°17'05
L16
L17
L1
L5
L2
L3
L6
L4
L10
L7
L9
L8
L13
L11
L12
L14
L15
N
300 m
46°16'40

Fig. 2

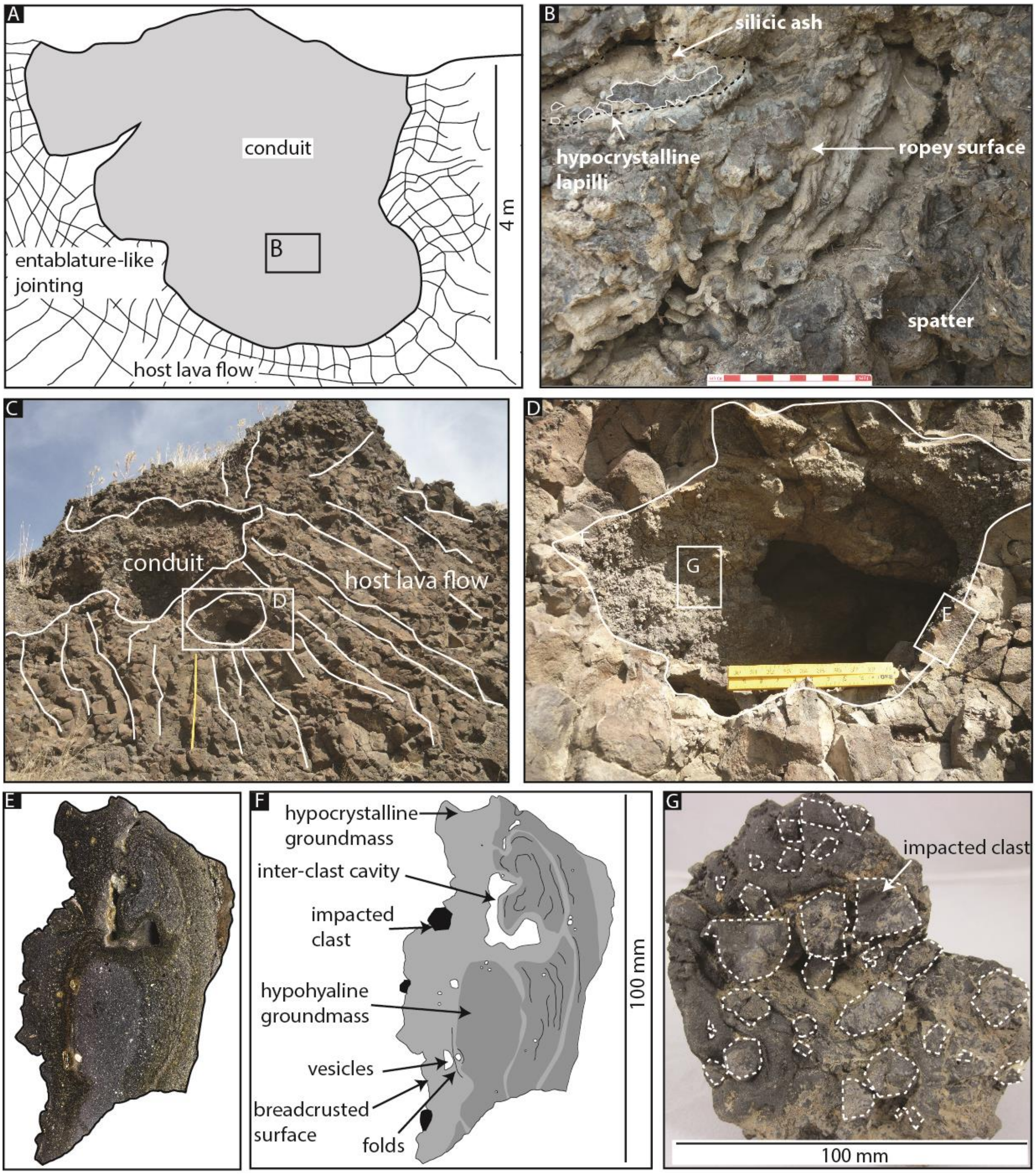
A
conduit
B
4 m
entablature-like jointing
host lava flow
B
silicic ash
hypocrystalline lapilli
ropey surface
spatter
C
conduit
host lava flow
D
D
G
E
E
F
hypocrystalline groundmass
inter-clast cavity
impacted clast
hypohyaline groundmass
vesicles
breadcrusted surface
folds
100 mm
G
impacted clast
100 mm

Fig. 3

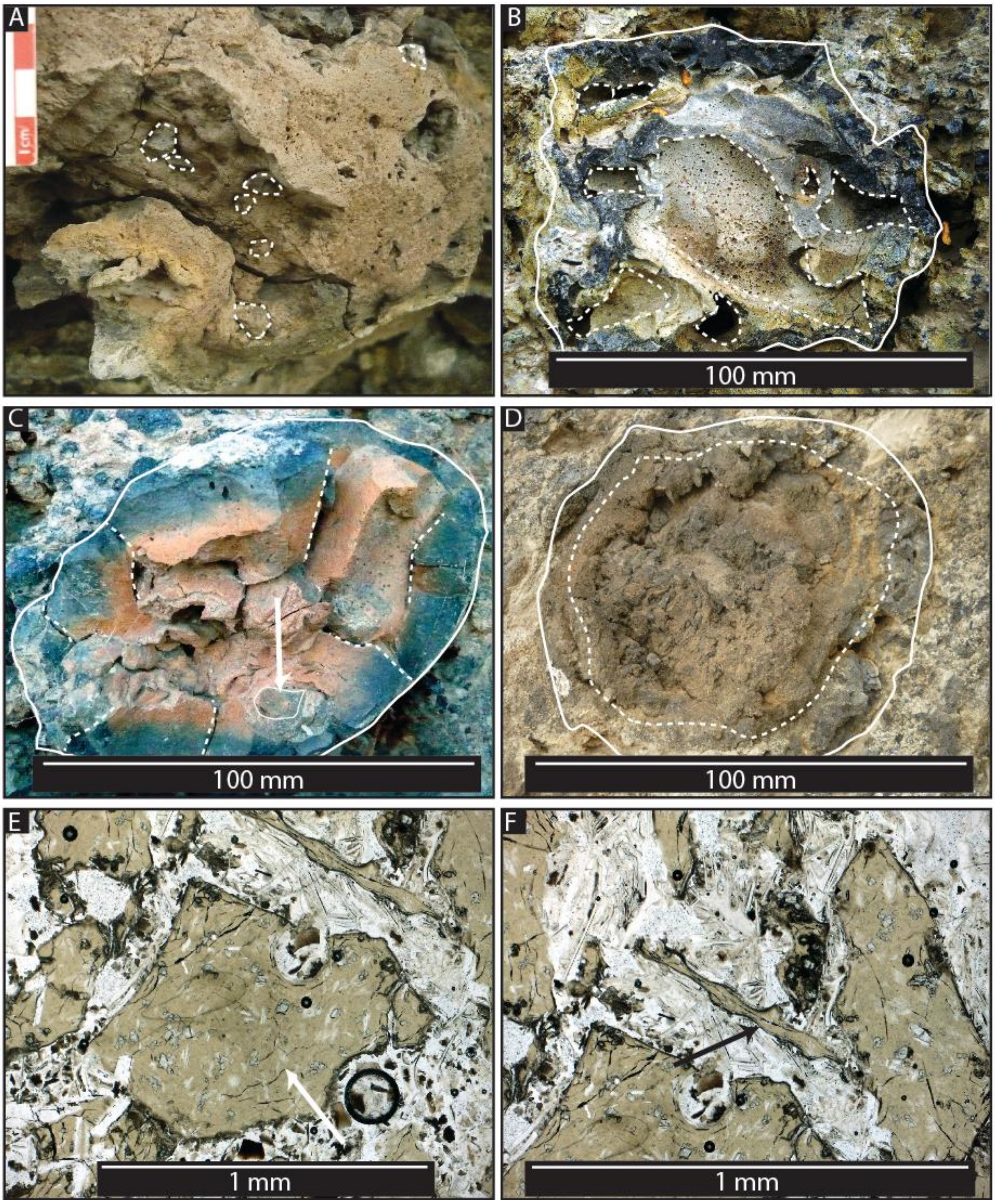

Fig. 4

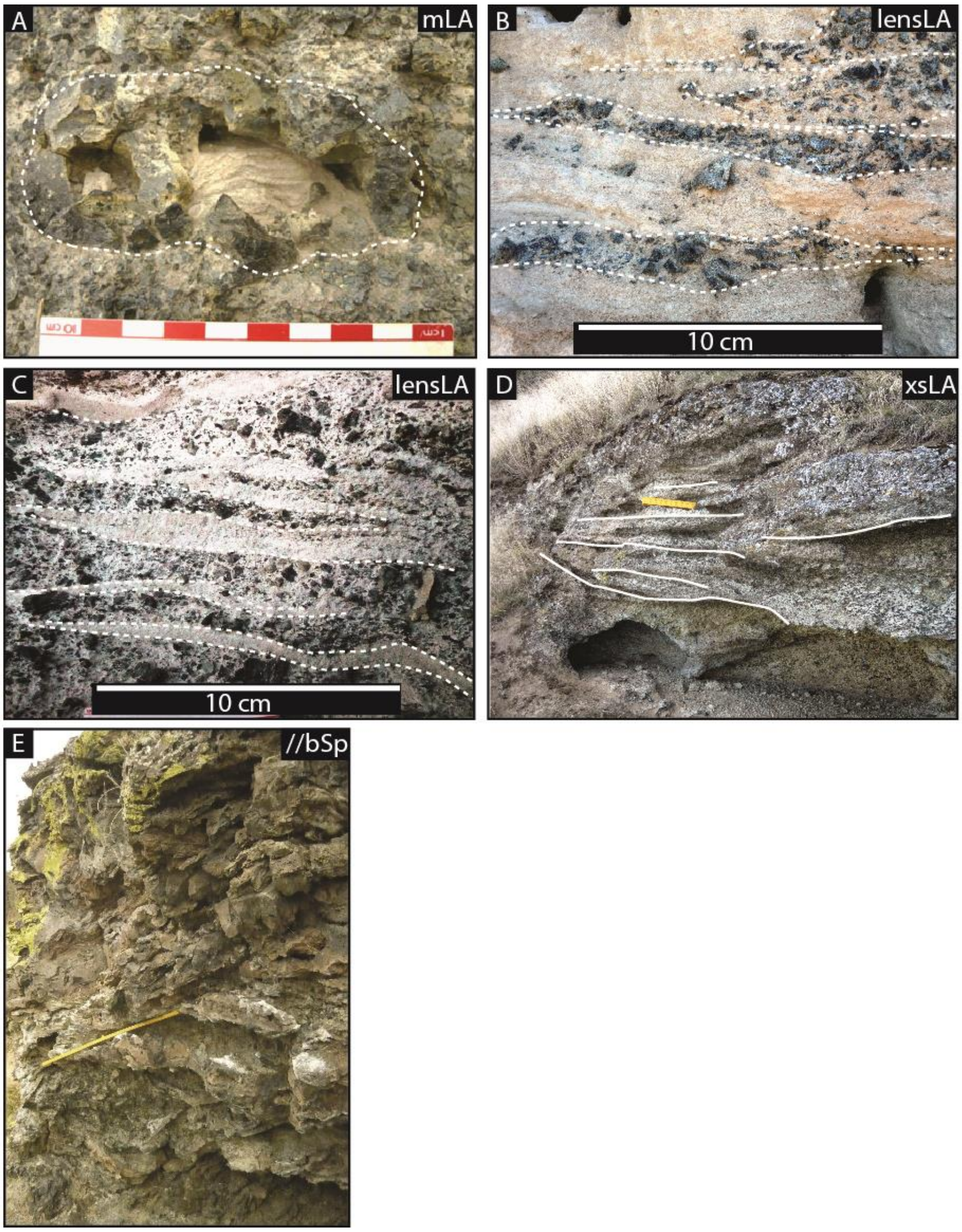

Fig. 5

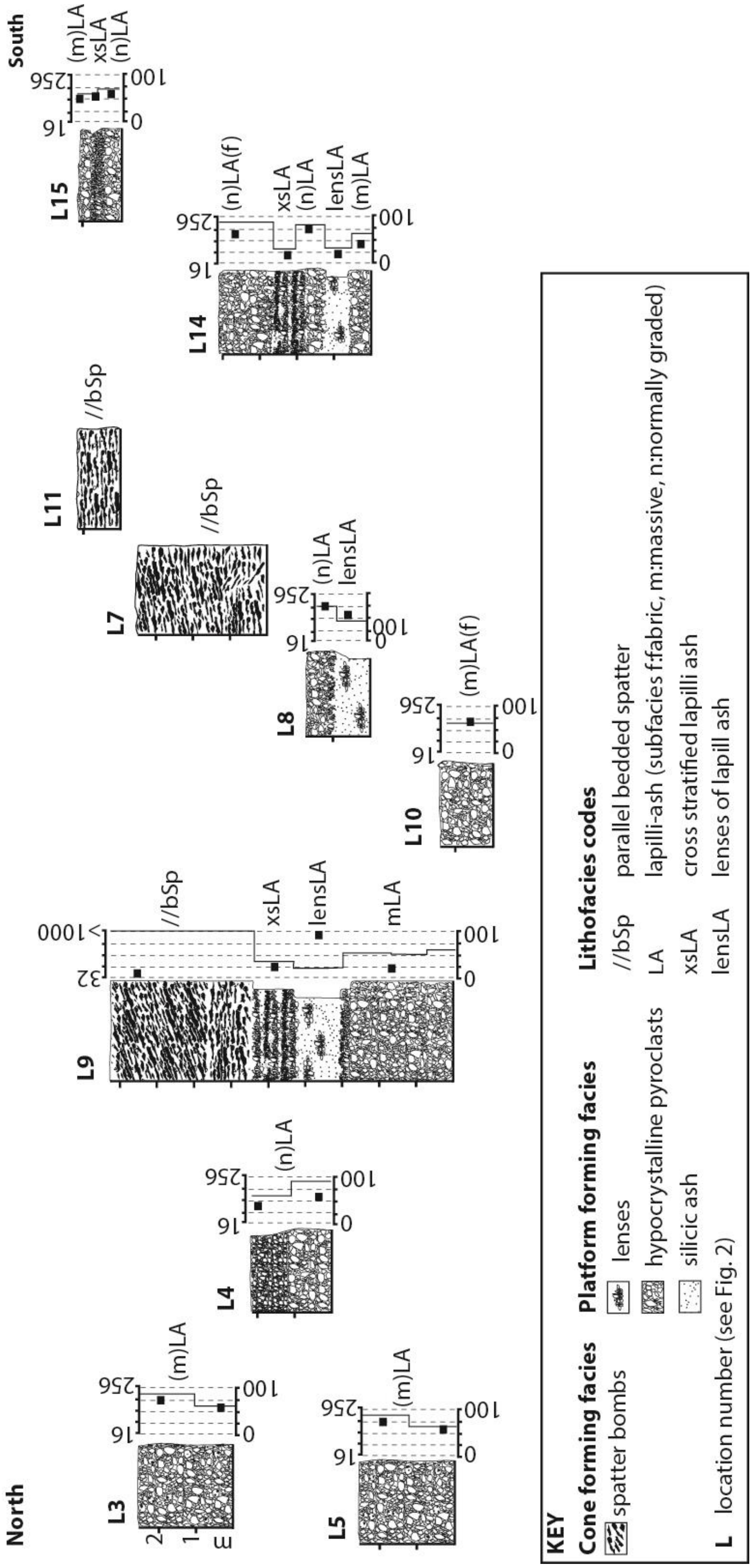
North
South
L3
L4
L5
L7
L8
L9
L10
L11
L14
L15
2
1
m
16
256
32
>1000
0
100
(m)LA
(n)LA
//bSp
xsLA
lensLA
mLA
(m)LA(f)
(n)LA(f)
KEY
Cone forming facies
spatter bombs
Platform forming facies
lenses
hypocrystalline pyroclasts
silicic ash
Lithofacies codes
//bSp parallel bedded spatter
LA lapilli-ash (subfacies f:fabric, m:massive, n:normally graded)
xsLA cross stratified lapilli ash
lensLA lenses of lapill ash
L location number (see Fig. 2)

Fig. 6

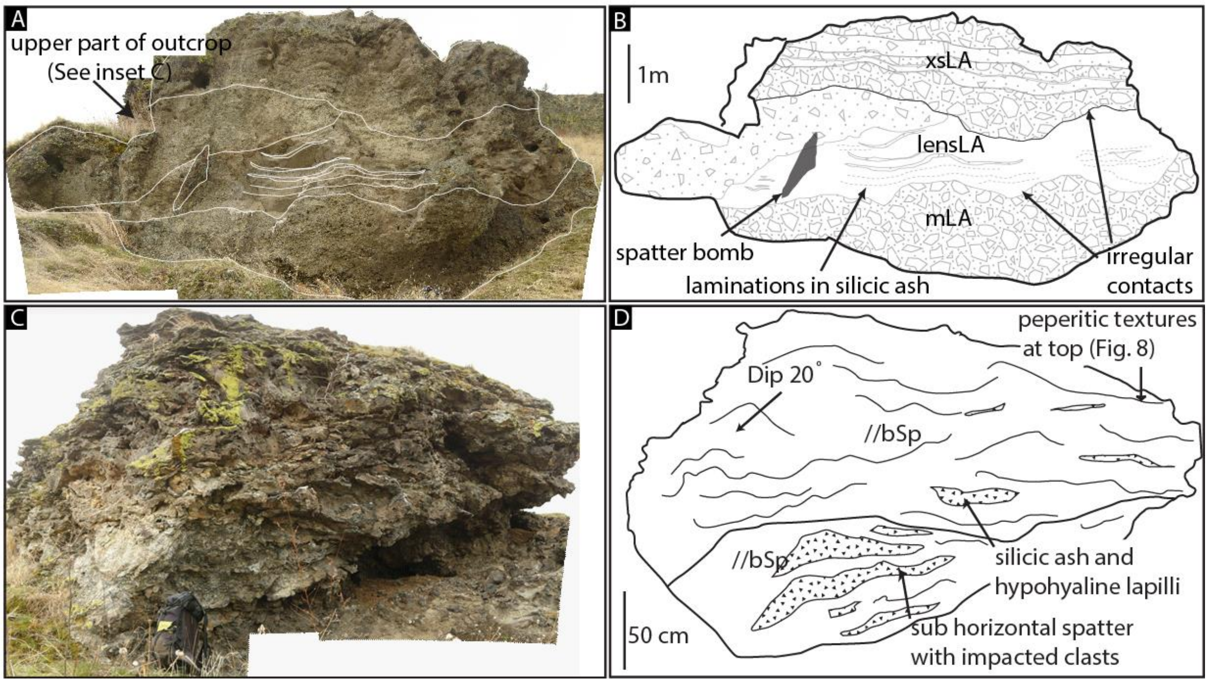
A
upper part of outcrop
(See inset C)
B
1m
xsLA
lensLA
mLA
spatter bomb
laminations in silicic ash
irregular
contacts
C
D
peperitic textures
at top (Fig. 8)
Dip 20˚
//bSp
//bSp
silicic ash and
hypohyaline lapilli
sub horizontal spatter
with impacted clasts
50 cm

Fig. 7

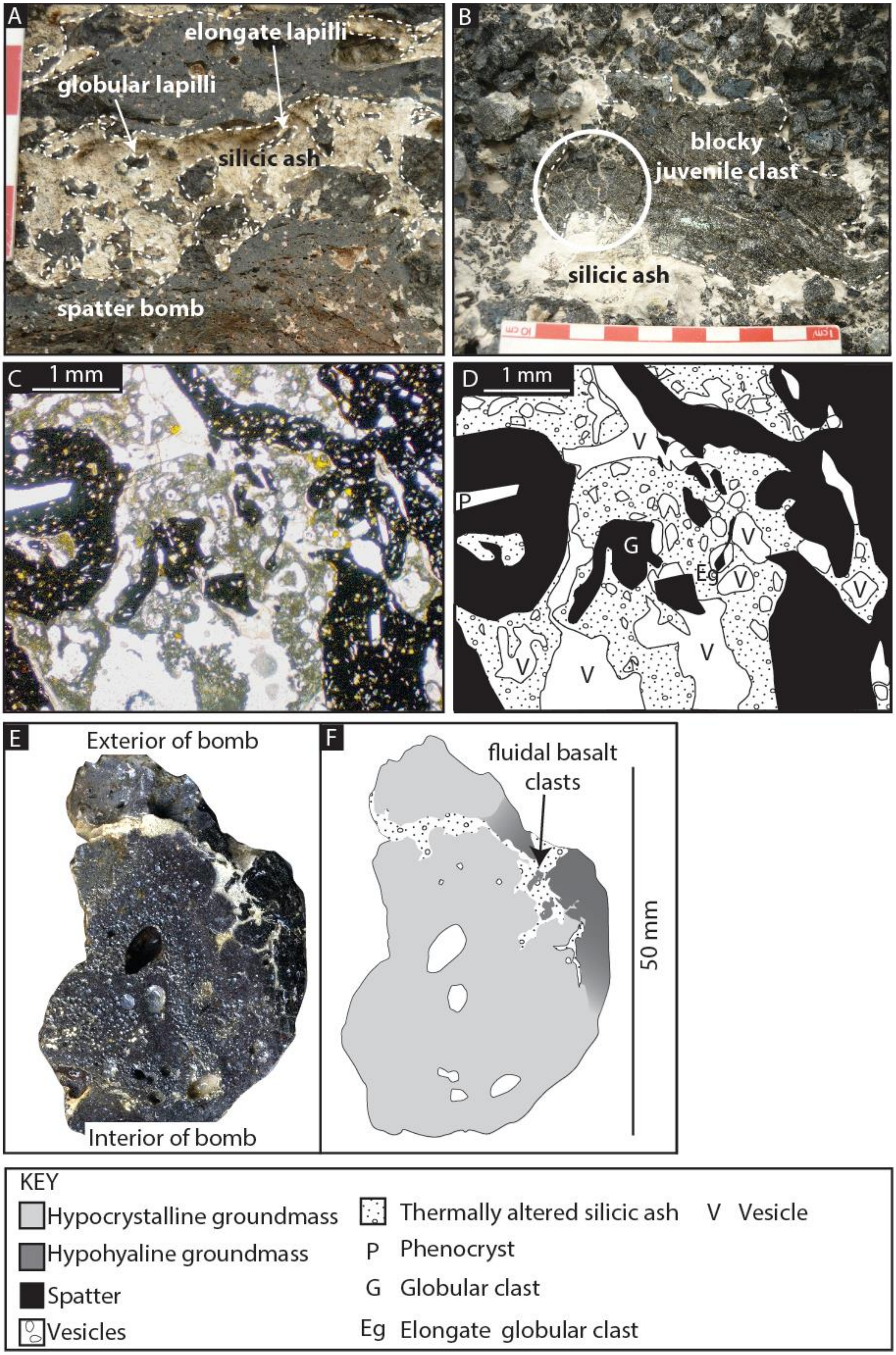
A
elongate lapilli
globular lapilli
silicic ash
spatter bomb
B
blocky juvenile clast
silicic ash
C
1 mm
D
1 mm
V
P
G
Eg
E
Exterior of bomb
Interior of bomb
F
fluidal basalt clasts
50 mm
KEY
Hypocrystalline groundmass
Hypohyaline groundmass
Spatter
Vesicles
Thermally altered silicic ash
P Phenocryst
G Globular clast
Eg Elongate globular clast
V Vesicle

Fig. 8

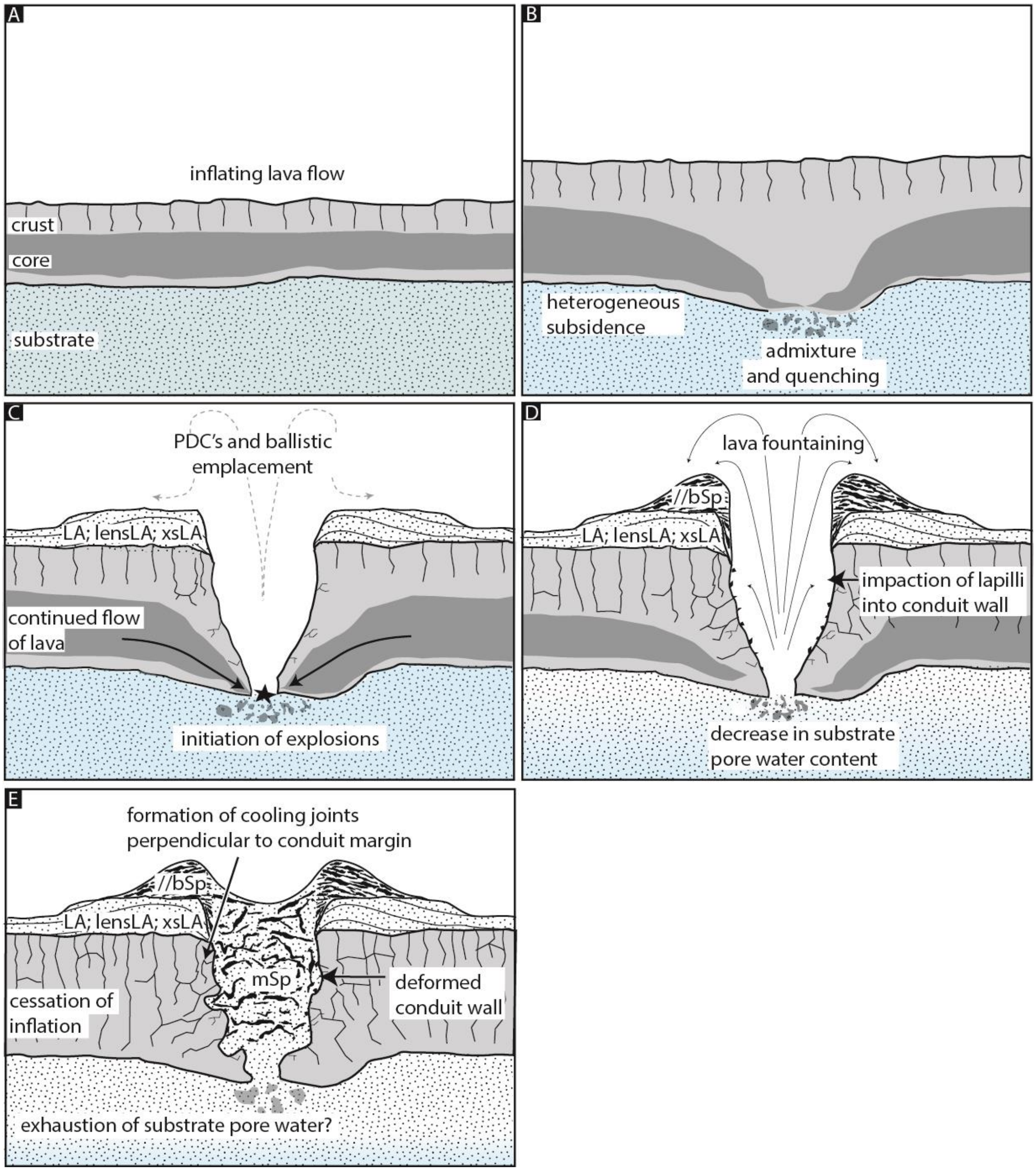
A
inflating lava flow
crust
core
substrate
B
heterogeneous
subsidence
admixture
and quenching
C
PDC's and ballistic
emplacement
LA; lensLA; xsLA
continued flow
of lava
initiation of explosions
D
lava fountaining
//bSp
LA; lensLA; xsLA
impaction of lapilli
into conduit wall
decrease in substrate
pore water content
E
formation of cooling joints
perpendicular to conduit margin
//bSp
LA; lensLA; xsLA
mSp
deformed
conduit wall
cessation of
inflation
exhaustion of substrate pore water?

Fig. 9

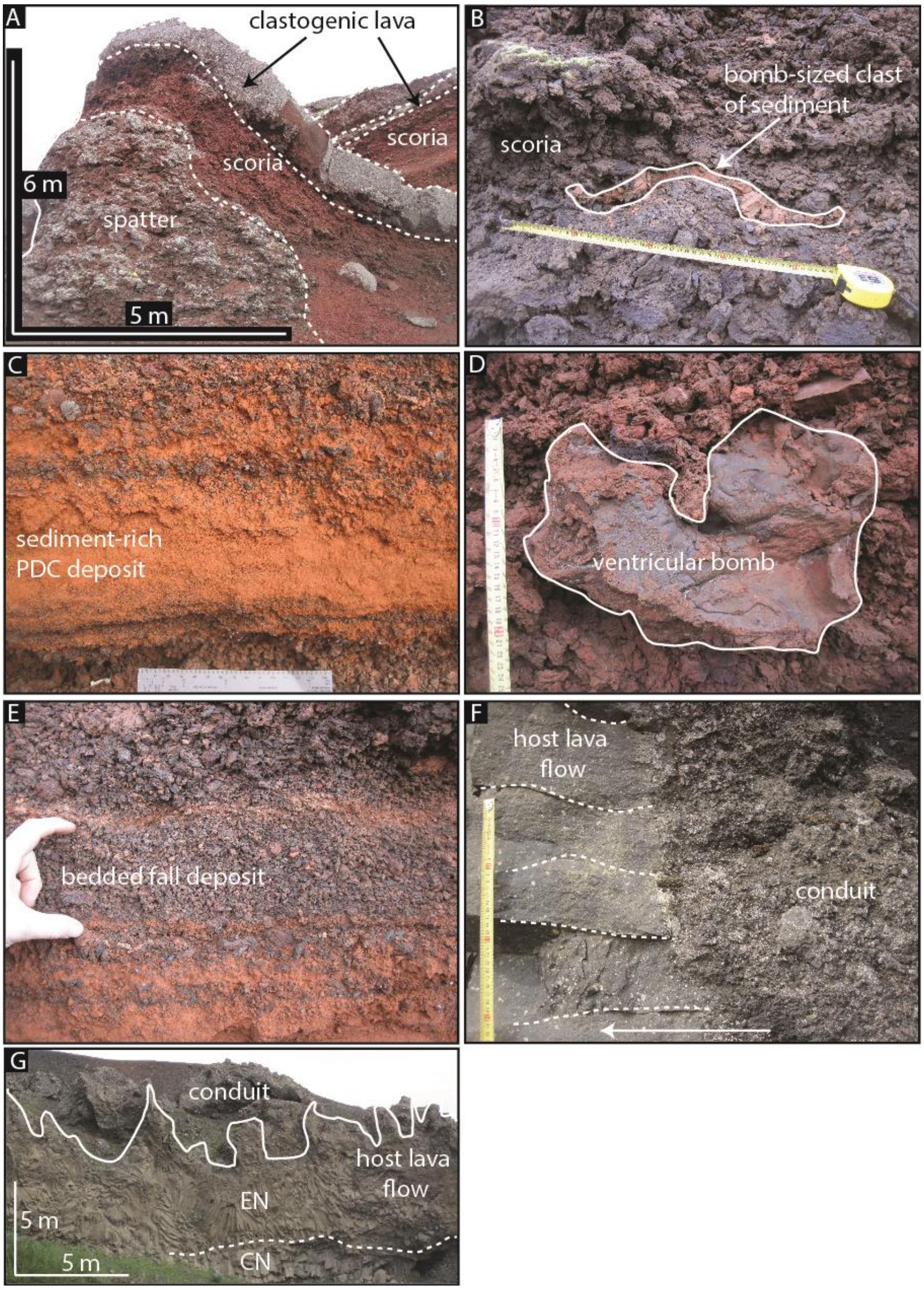
A
clastogenic lava
scoria
scoria
6 m
spatter
5 m
B
bomb-sized clast of sediment
scoria
C
sediment-rich PDC deposit
D
ventricular bomb
E
bedded fall deposit
F
host lava flow
conduit
G
conduit
host lava flow
EN
5 m
5 m
CN

Fig. 10